Detailed Technical Progress Report

Details of Milestone under consideration (with the scheduled time of completion and status /progress of all technical activities):

Month Of End Of Activity	Objectives	Activities *(as mentioned in the final GLA signed)*	Status *(For more details, please refer to detailed work done below)*
3	**Wheelchair Prototype Design and Fabrication + EEG Headset Testing**	CAD design of new mounts (for new onboard computer, EEG headset stand with wire holders, reclining feature) and features in wheelchair and Fabrication of the wheelchair prototype	**Achieved** (Refer section-1.1). Fully functional motorized wheelchair fabrication achieved with a standard base chassis. Required sensors are mounted with custom 3D printed mounts and onboard computing platform attached. wheelchair ready for navigation.
5		BCI Training and Testing of MND Patients in a robotic arena, vis-à-vis describing experiments and basic instructions of thought to the subjects. Voice based control command generation and training models for voice to text.	**Achieved.** 1. 20 healthy subjects data were collected for BCI. (Refer section -1.2.1) 2. Data collection and analysis done on three MND patients. (Refer section -1.2.5) 3. BCI and voice based testing done on healthy subjects. (Refer section-1.3).
6		Fully manufactured system with design and electronic integration. EEG system integration established	**Achieved.** (Refer section-1.4). EEG system integrated with wheelchair via PC. Standalone system needs to be done.

8	**Sensor integration & Control module Testing in an indoor environment.**	Obstacle Avoidance simulation and real time testing of a path planning algorithm for Wheelchair.	**Achieved** (Refer section-2.1, 2.2 & 2.3). 1. Achieved 3D mapping, static and dynamic obstacle avoidance in simulation and in the lab environment. 2. Conducted real-time path-planning in lab environment using Dijkstra's and Dynamic Window Approach path planners.
10		Integrating BCI control with sensors and path-planning algorithm for the wheelchair.	**Achieved** (Refer section-2.4). Integrated real time EEG based control for waypoint based navigation in a virtual reality environment, with subject and session independent testing.
11		Indoor environment testing for a real time task to check if BCW subject can navigate along the desired trajectory effectively. Initiating Voice based control command generation and training models for voice to text in an indoor environment	**Achieved** (Refer section-2.5). All modules tested independently. Realtime wheelchair testing with healthy subjects' data was performed.
12		Wheelchair ready for navigation. Self mapping and navigation with path planning.	**Achieved** (Refer section-2). 1. Achieved 3D mapping, static and dynamic obstacle avoidance in simulation and in the lab environment. 2. Conducted real-time path-planning in lab environment using Dijkstra's and Dynamic Window Approach path planners.
14	**Task Optimization and Multi-Scenario Testing**	Outdoor testing BCI adaptation to navigate around unknown environments like cycle lanes and parks Optimization of the BCI algorithm Voice based control command generation and training models for voice to text in outdoors.	**Achieved** (Refer section-3). 1. Outdoor testing for the wheelchair is currently being done. 2. Testing of BCI on disabled patients have been carried out.

15		Beta testing with healthy elderly and impaired subjects followed by final prototype	**Achieved** (Refer section -1.2) MND movement restrictive patients EEG data for BCI were collected during clinical visits and analyzed for final prototype.
16		Beta testing with 10 healthy elderly and impaired subjects at 2 clinical centers, Inclusion of safety features for the flawless and safe usage by both healthy elderly and impaired subjects. **Revised Objective:** As project is ending, focus should be to get at least 1-2 patients with motor deficit and have their EEG and either virtual or wheelchair control mapped. That would show the real challenge. (TEC recommendations)	**Achieved** 1. 20 healthy subjects data were collected for BCI. (Refer section -1.2.1) 2. 3 MND patients data were collected for prototype check and analyzed. (Refer section -1.2.5) 3. Inclusion of safety features for the flawless and safe usage by both healthy elderly and impaired subjects completed.
17		Tested prototype ready for manufacturing	**Achieved** Wheelchair prototype is partially ready for manufacturing concerning outdoor environment.

Detailed Work done:

1 Objective 1: Wheelchair Prototype design and fabrication with EEG headset

1.1 Objective 1.1: CAD design of new mounts (for new onboard computer, EEG headset stand with wire holders, reclining feature) and features in wheelchair and Fabrication of the wheelchair prototype

- Fully functional motorized wheelchair fabrication achieved with a standard base chassis.
- Required sensors are mounted with custom 3D printed mounts and onboard computing platform attached. Wheelchair ready for navigation.

1.1.1 CAD Designs of Different Modules

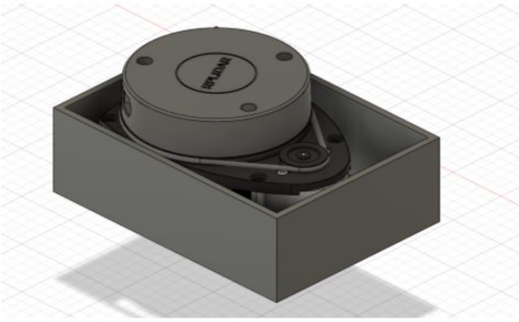

(a) LIDAR Mount.

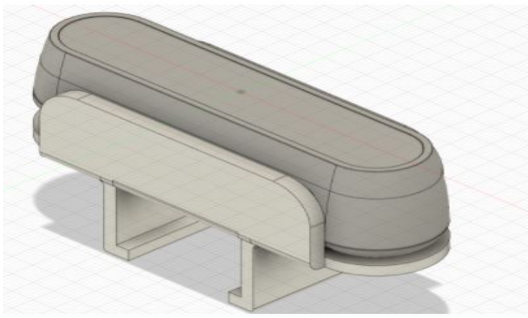

(b) Depth Camera Mount.

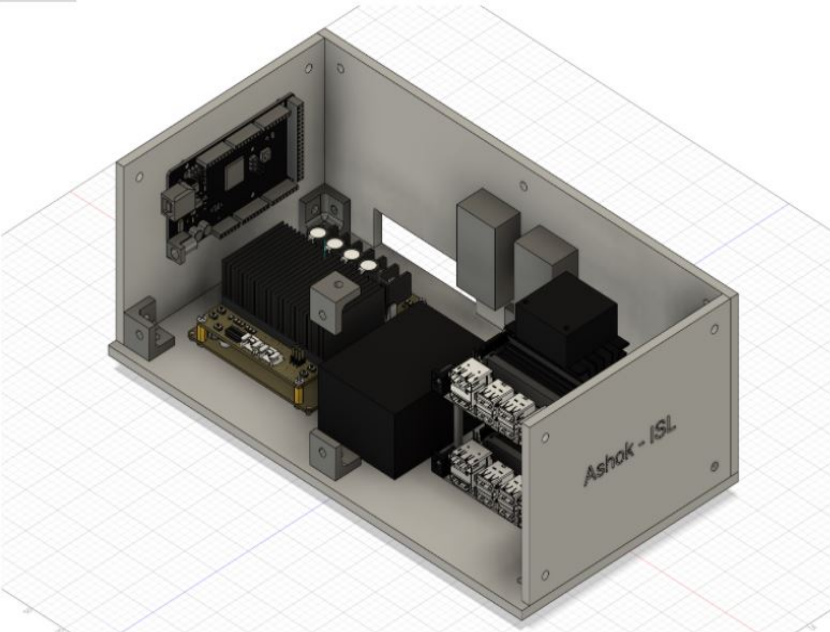

(c) Control and Power Management Box.

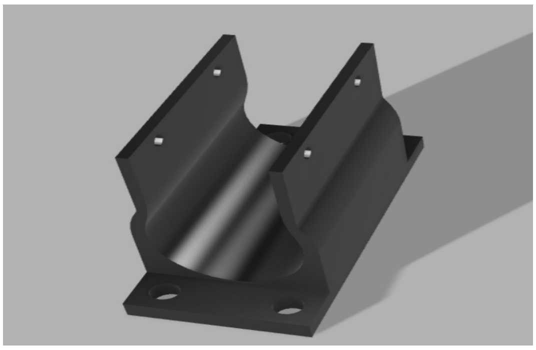

(d) Encoder Holder.

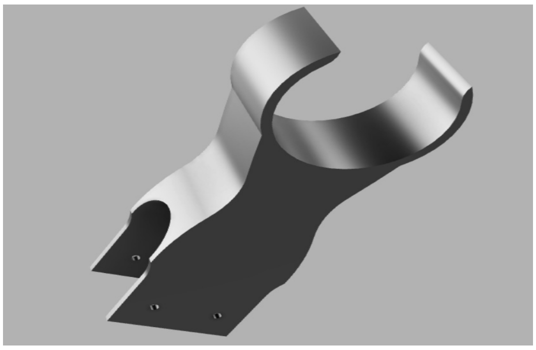

(e) Encoder Holder.

1.1.2 Features in wheelchair and Fabrication of the wheelchair prototype

- **Wheelchair Robot hardware description:**

1. Dimensions: 114 x 64 x 93.5 cm
2. Frame Material: Iron
3. Wheelbase: 13" Diameter
4. Drive Type: Differential Drive
5. Weight without Sensors: 45 Kilograms
6. Battery: 24V. Capable of driving around 15 km on a full charge.
7. Max Load Carrying Capacity: 100 kg (with sensors)
8. Motors: 2
9. Drive range : 20 km on a full charge.

- **Sensors Used and Components Used:**

S.No	**Name**	**Description**	**Image**
1.	Intel RealSense D435i	Depth Camera	

2.	RPLidar A1	LIDAR	
3.	RAZOR 9DOF AHRS System	IMU + AHRS	
4.	Autonics Encoders	Encoder	
5.	Jetson Nano	Computing Devices	
6.	Arduino Mega	Microcontroller	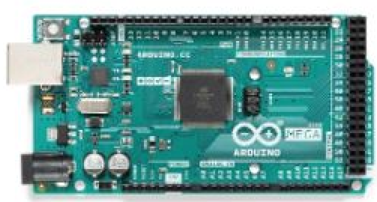

7.	Waveshare 7" Touch Display	Onboard Display	
8.	Control and Power Management Box	For controlling and managing different power levels and battery management and fail-safe system	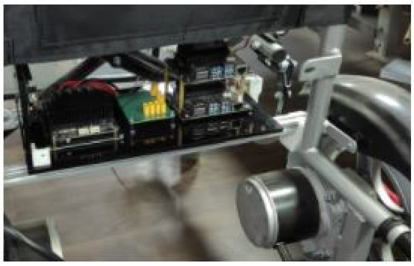
9.	BCI Cap	An OPENBCI Ultracortex mark 4 EEG headset is used for signal acquisition, and an OPENBCI Cyton bio sensing board to sample and feed the EEG signals over bluetooth to the main computing device.	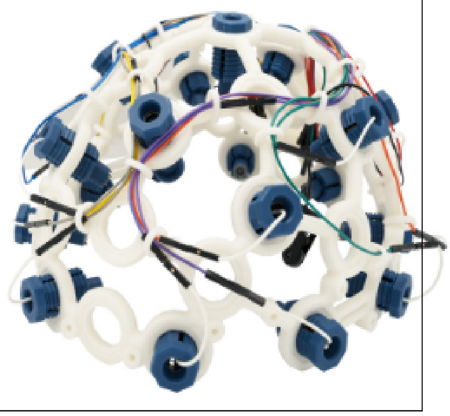

1.1.3 Compute Capabilities

- **NVIDIA Jetson Nano:** It is a full Linux computer capable of running ROS (Robot Operating System)[1]. It has 4GB of LPDDR4 memory with Bluetooth and Wi-Fi. It's GPU has 128 CUDA cores based Maxwell architecture while CPU is Quad-core ARM Cortex-A57 MPCore. It has 4x USB 3.0 and 1x USB 2.0 Micro-B ports with GPIO, I2C, I2S, SPI, UART and Gigabit Ethernet connectivity. The Jetson Nano also provides a compact form factor, allowing it to be easily embedded with the wheel chair. At peak it only consumes 20W keeping the power demand low.

- **Intel NUC Mini PC:** A quad core 8th gen Intel Core i5-8259U NUC is used as main PC which drives the touch display, capture and process the 3D depth cloud data. The RAM is 16GB DDR4 at 2400Hz and the main drive is 256GB SSD. It has 4x USB 3.1 gen2 ports and 2x USB 2.0 internal ports with Gigabit Ethernet connectivity. It runs on 19V.

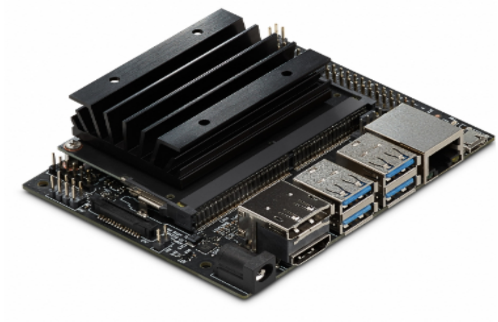

(a) Jetson Nano

(b) Intel NUC

Figure 2: Computation Devices.

1.1.4 Communication Infrastructure

Communication among sensors, actuators, display devices, and compute modules has been designed in a modular way to achieve active load balancing. The system is easy debuggable and repairable. The overall sensor interface and network communication infrastructure is given in the Fig. 3.

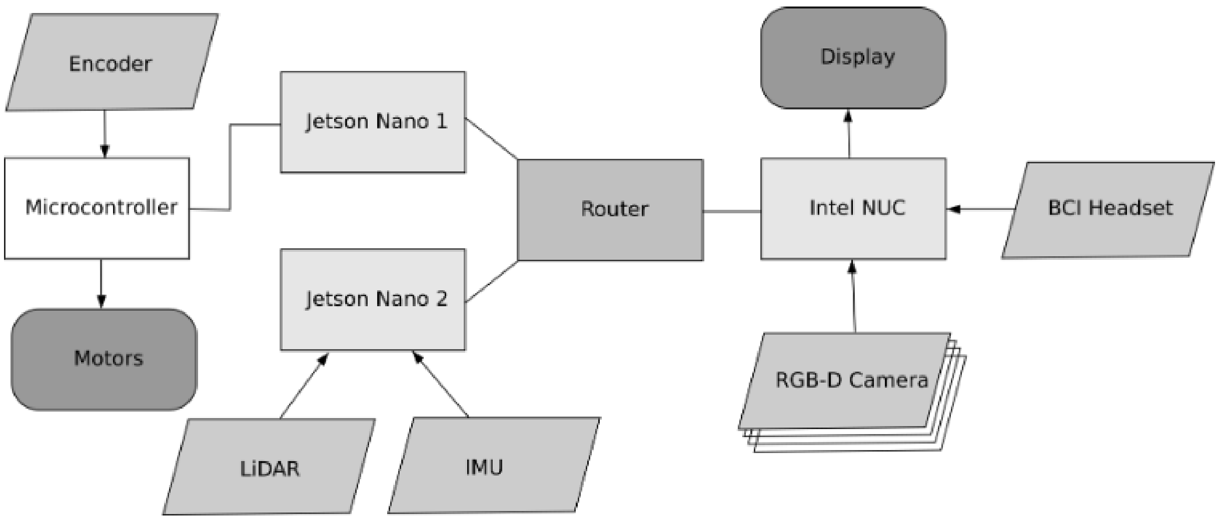

Figure 3: Sensor Interface and Network Communication.

The display flashes probable destinations where the wheelchair can navigate. The destination goal is captured from the brain by the BCI headset. It transfers this information to the Intel NUC wirelessly through Bluetooth, where path planning algorithms use it to plan the path. The feedback from sensor data fusion from the camera attached to NUC, *LiDAR* and IMU hooked to Jetson Nano 2 and encoders attached to Jetson Nano 1 are used by the system to generate forward and angular velocity for the wheelchair. These velocities are sent to the microcontroller connected to Jetson Nano 1 via serial interface, converting to individual wheel velocities set by the motor driver. All three computing devices are connected through a router via ethernet.

1.2 Objective 1.2: (a) BCI Training and Testing of MND Patients in a robotic arena

1.2.1 BCI Training and Testing of healthy patients

A brain-computer interface (BCI) is a computer-based system that acquires brain signals, analyzes them, and translates them into commands that are relayed to an output device to carry out a desired action. In principle, any type of brain signal could be used to control a BCI system. The most commonly studied signals are electrical signals from brain activity measured from electrodes on the scalp, on the cortical surface, or in the cortex. A BCI system consists of 4 sequential components:

1. Signal acquisition,
2. Feature extraction,
3. Feature translation,
4. Device output

These 4 components are controlled by an operating protocol that defines the onset and timing of operation, the details of signal processing, the nature of the device commands, and the oversight of performance.

1. **Motor imagery:** Motor imagery (MI)–based brain-computer interface (BCI) [2] is one of the standard concepts of BCI in which the user can generate induced activity from the motor cortex by imagining motor movements without any limb movement or external stimulus. If the user is asked to perform a right hand motor imagery, he/she will imagine that he/she is moving his/her right hand, which will translate in a potential drop of the left part of the brain (C3 position) and a left hand motor imagination will lead into potential drop in right side of the brain (C4 position). These changes in potential between different parts of the brain can be used to classify into left and right hand motor imagination. In the training session, the experimenter collects each user's MI data, does feature extraction with them, and makes classification algorithms through the data collected. During the testing session, algorithms already trained are applied to new MI data for classi!cation on a real-time basis. In this case, if we correlate the user going forward with a right hand motor imagery, the user will have to perform a right hand MI to move forward.

2. **P300:** A P300 brain-computer interface (BCI) [3] is a paradigm, where text characters are decoded from event-related potentials (ERPs). In a popular implementation called P300 speller, a subject looks at a display where characters are flashing and selects one character by attending to it. The selection is recognized as the item with the strongest ERP. The speller performs well when cortical responses to target and non-target stimuli are sufficiently different. We have modified this approach to use it for selecting destinations and implementing home automation. Suppose there are 3 rooms and the user wants to go to Room 1, then room 1 will act as the target and the other two will be non-targets. Similar paradigms can be set between various home appliances to establish home automation.

1.2.2 BCI Approach-1:

We utilized the motor imagery approach specifically for the navigation purpose and P300 for both navigation and automation purposes, we had to integrate the characteristics of both the scenarios. For Motor Imagery, we have trained and tested on 20 subjects (age 22-35 years). And for the P300 paradigm, we have trained and tested on 8 subjects (age: 24-32 years).

- **Electrodes and Devices:** Our approach focuses on a lesser number of active electrodes (Maximum of 8). We had selected 4 electrodes for each of MI and P300 paradigms. For MI, we have used C3, C4, CP1, CP2 which obtains best MI information, and for P300 we have used P3, P4, Pz and Cz. Additionally two electrodes were used in FP1 and FP2 positions to obtain any artifacts caused by eye blinking and cancelling out the trials, so that better quality of data will be fed during training. We have used a OPENBCI Ultracortex mark 4 EEG headset for signal acquisition, and an OPENBCI Cyton biosensing board to sample and feed the EEG signals.

- **Experimental Paradigm:** A closed indoor environment was chosen to conduct the training session for both Motor Imagery and P300 paradigms. Outside noises and external disturbances were limited and were avoided as much as possible to increase the attention level of the subjects. In the room, a Television Screen was kept in front of the subjects which provided the necessary cues.

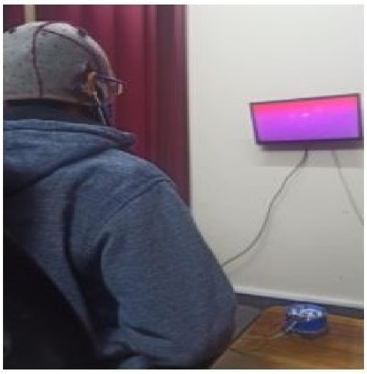

- **Motor Imagery:**
  - **Signal and Data Acquisition:** For the training of MI, we have chosen 20 subjects and each subject has gone through 2 Offline or training sessions and 2 online and testing sessions. For the training sessions, we have asked the subjects to perform 3 kinds of motor imagery, Right Hand, Left Hand and Both Feet. Out of these three, we calculated classification accuracy of each pair after training with the data and obtained which pair performed the best. During training, for each training session, there were 3 runs. In each run, we had 15 trials for each kind of MI (i.e total 45). Each trial was 12 seconds long. After the training session, we obtained the best fit pair for each subject and used only those two kinds of MI for the testing session. Each testing session consisted of 3 runs. Each run consisted of 15 trials of each MI class. Before the beginning of the experiment as well as after each session, we asked a few questions to each subject about their physical state, mental state, attention level and expected accuracy etc.The timeline of a single trial and the Event Related Desynchronization for a subject pattern are given in figure 5.

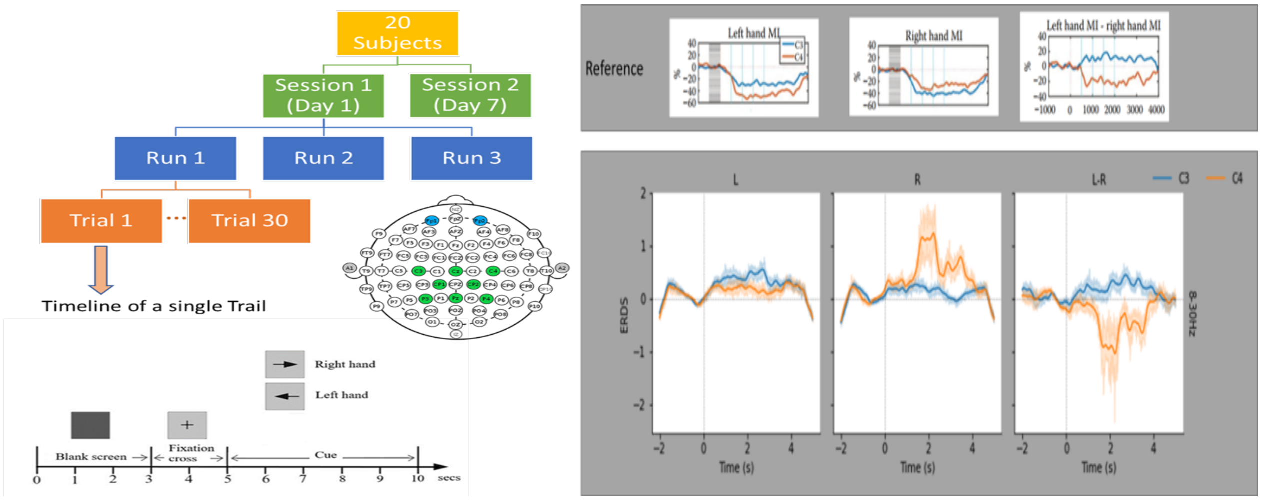

Figure 5: Left: Data collection sequence and timeline of a single trial. Right: ERD (Event Related Desynchronization) pattern obtained for a single subject.

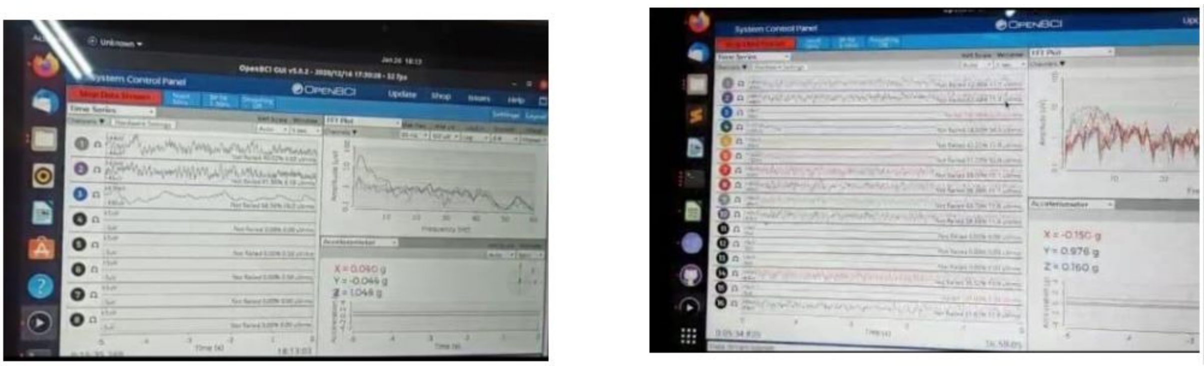

Figure 6: Graphical user interface for date acquisition.

– **Feature Extraction and Classification:** The time series and frequency spectrogram of the collected healthy subjects data are shown in figure 7. The relevant brain information for MI are available in the range of 8-30Hz. Hence suitable frequency filters are employed to extract these rhythms.

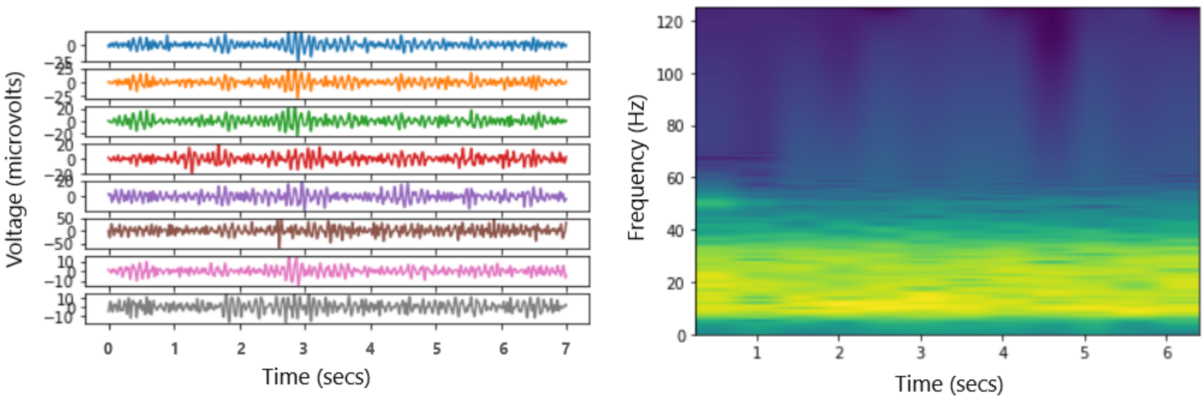

Figure 7: Time series and frequency spectrogram during MI.

After preprocessing the data, we have used two different kinds of feature extraction methods, Riemannian Geometry and Common Spatial Pattern. The pipelines comprises of both Riemannian based classifiers such as Minimum Distance to Mean (MDM), Fishers Geodesic MDM (FGMDM), Riemannian tangent space features with Support Vector Machine (SVM), Linear Discriminant analysis (LDA) and Common Spatial Pattern (CSP) features with to SVM and LDA classifiers. The results of the top best 10 subjects using seven clasiifier pipelines are shown in figure 8.

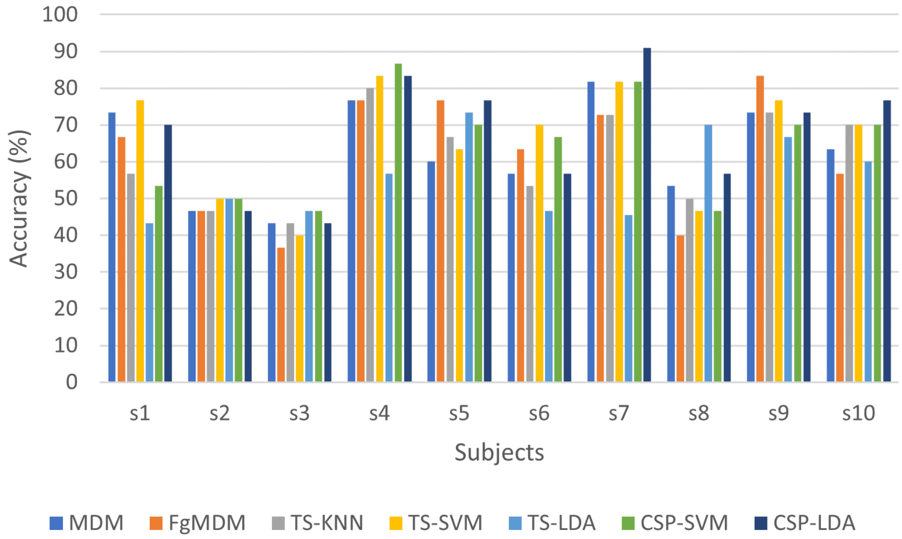

Figure 8: MI accuracy results of the best 10 healthy subjects.

Further, we have explored the use of an adaptive approach over the Riemannian Geometry based method which minimized the non-stationarity and noise in EEG signals, and fed well formed features to the classifiers which resulted in a better classification accuracy [4]. Despite being one of the most popular feature extraction algorithms, Common spatial patterns are known to be very sensitive to noise and produce large inter subject and inter session variances. To overcome this issue, we have used 4 different kinds of Regularized CSP algorithms which not only outperformed the CSP in Classification accuracy but performed more efficiently subject to subject transfer. Upon comparing both the features, we concluded that Riemannian based adaptive features work better than the Regularised Common Spatial Patterns. Inter session accuracy for subjects increased from 55 to 75 percent (mean accuracies across all subjects) upon using Adaptive Riemannian over Common Spatial Patterns.

- **P300 based paradigm:**
  - **Data Acquisition:** For P300, we had two different kinds of scenarios, one for navigation and another for home automation. For navigation, we have selected 6 rooms, out of which one will be target and rest will be non-targets. We have collected the EEG signals for both the Target data and Non-target data and used it to classify. Similarly, for home automation, we have used 6 Basic home appliances such as Light, Fan, AC etc. Out of those, one was the target and the rest were non-targets and we proceeded as described earlier.

    We have conducted two sessions for both Navigation and Automation. In each session, there were 4 runs. In each run, there were 120 trials (approximately 20 targets and 100 non-targets).

Each trial consisted of 0.9 sec (0.4 sec of cue and 0.5 of blank screen).

Before the beginning of the experiment as well as after each session, we asked a few questions to each subject about their physical state, mental state, attention level and expected accuracy etc.

– **Feature Extraction and Classification:** After collecting the data, We have tried to use Filter Bank Common spatial pattern (FBCSP) based features and Tangent space based Riemannian Geometry features. We have observed Riemannian Geometry does not work well in P300 paradigms whereas FBCSP based features provided well classification accuracies after classifying through DNN. For Navigation, We have achieved a Mean Accuracy of 83.33%.

1.2.3 BCI Approach-2:

- **Our methods:** We utilized the motor imagery approach specifically for the navigation purpose for both navigation and automation purposes. After benchmarking existing approaches, we have developed a novel motor imagery based intent recognition algorithm with minimal sensor (EEG channels) usage and real time predictions. Tested and benchmarked for 10 subjects across multiple sessions. This algorithm provides for reliable session independent prediction of intent across subjects.

- **Electrodes and Devices:** Our approach focuses on a lesser number of active electrodes (Maximum of 5). We had selected 4 electrodes and a cumulative bias. We have used C3, C4, CPZ, CZ. In the future, two electrodes may be added at FP1 and FP2 positions to obtain any artifacts caused by eye blinking and head ag cancelling out the trials, so that better quality of data will be fed during training. We have used a OPENBCI Ultracortex mark 4 EEG headset for signal acquisition, and an OPENBCI Cyton biosensing board to sample and feed the EEG signals in real time.

1.2.4 Proposed Session independent BCI Approach (online dataset)

the EEG pattern of the user for the same MI task changes over time due to changes in the user's psychophysiological state and the shift in electrode placements over the sessions. This cross-session variability makes the practical use of BCI challenging, as a separate calibration procedure is required to tune the decoding model for each new session. This procedure of collecting EEG data for re-training is time-consuming and tiring for the user. Hence, approaches to reduce the calibration time or eliminating this procedure will aid in more practical applications of the BCI systems. Multiple approaches based on transfer learning have been adapted in literature [5]. Based on our findings, we have proposed a session independent adaptive Riemannian feature based framework to handle the session-to-session variance.

From the EEG trials, the best time window of signal extraction and best 'K' filter bands are calculated based on Riemannian distance-based 'Dscore' metric. The spectral filtered EEG trials' covariance matrix in multiple frequency bands are affine transformed to align it with the baseline reference covariance matrix using Riemannian Geometry concepts. The transformed covariance matrices in selected spectral bands are FGDA filtered using Riemannian Tangent Space concepts. Finally, the transformed FGDA spectral covariance matrices are given input to the CNN model, which integrates the features from the different spectral regions. The entire framework is given in figure 9.

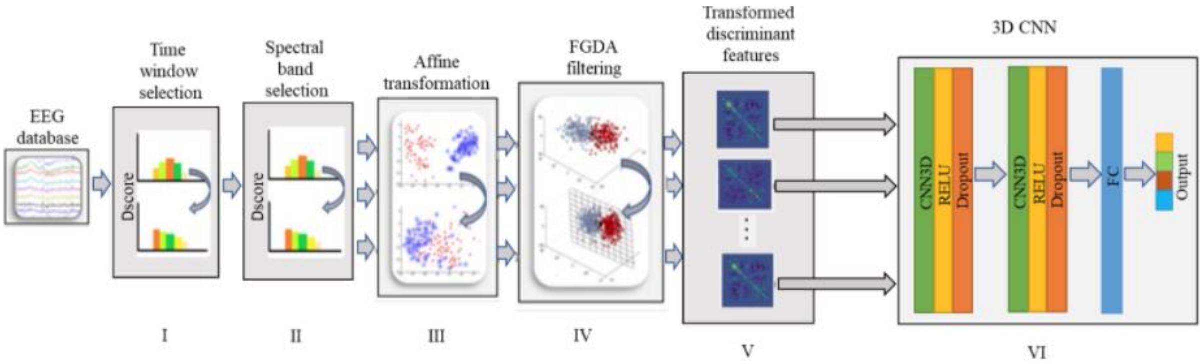

Figure 9: The EEG data are extracted in the best time window and filtered in the selected filter bands using the Dscore metric in stages I and II respectively. In III, the spectrally filtered trials are affine transformed to make the different sessions data comparable and are FGDA filtered in IV. V shows the transformed FGDA filtered covariance features in selected spectral bands which are given as inputs to the CNN model in VI.

To generate a robust adaptive feature representation of incoming EEG data and to utilize the extracted features in classification, we have contemplated the following points:

1. Extract the best bands and time window based on discriminant patterns in the diverse spectral bands and time windows of the EEG data.
2. Utilize the nonlinear and spatial information contained in the covariance format of EEG signal.
3. Facilitate cross-session learning to skip calibration procedure and also to adapt to the learned user patterns upon subsequent runs.
4. Incorporate a neural network model for classification instead of a linear classifier to capture the discriminative nonlinear features distributed in the data.

1.2.5 Disabled/movement restrictive patients

We have worked with three movement restricted patients to check for the presence of discriminative EEG patterns during movement imagination in order to drive the autonomous wheelchair. The patients consist of 2 male and 1 female who suffer from motor neuron disease. The patients were elaborated with the data collection procedure and their consent is taken before the start of the motor imagery experiments. The signed consent form of all the patients are available in appendix **??**. The offline EEG data of the three patients were collected under the supervision of *Dr. Rajeev Kainth, Neurosurgeon, Kainth's Brain and Spine clinic, Kanpur.*

- **Patient details:** The first patient P01 is 72 years old, male, right handed and is hemiparetic with his right side being completely disabled. Further, the patient had trouble communicating as his facial muscles were also affected and he required complete assistance for movement.The second patient P02 aged 52 years, male, right handed is affected by quadriparesis, a condition which weakens all the four limbs (both legs and arms). He could communicate well but relies on hand support for movement. The third subject P03 is a 30 year old female, right handed patient diagnosed with cerebral vascular accident (CVA) commonly referred to as stroke which results due to the interruption of blood flow to the brain cells. She is unable to move her right hand and has restricted movement in her legs. A picture of the patients during the experiment session is shown in figure 10.

Figure 10: Data collection of movement disabled patients.

- **MI experimental study on MND patients:** The study encompasses two stages: Electroencephalograpy (EEG) data collection and analysis of data. In the first stage of collecting data from Motor Neuron Diseased (MND) patients, EEG is used to capture the brain patterns when the subjects imagine left-hand and right-hand movements. The EEG data are then analyzed to check for the discriminability between the two tasks for the feasibility of a Brain-Computer Interface (BCI) system.

  Before collecting the EEG data, the patients along with their family members were explained in detail about the data collection procedures and the nature of study and asked to fill the consent form. The following are the steps involved in the first stage of data collection:

  1. The subject is asked to sit comfortably facing a monitor in which the visual instructions are displayed.
  2. The EEG headset from Openbci ultra-cortex is placed on the subjects head and adjusted for sufficient contact of the electrodes on the scalp till we get good signals.
  3. The experiment starts with the display of a focusing cross '+' upon which the subject waits for the cue with attention.
  4. After two seconds, a cue indicating right/left hand movement is displayed upon which the subject begins to imagine moving his right/left hand accordingly for five seconds.
  5. A three second rest period is then provided after which the procedure repeats using random cues. This entire timeline for a single trial is displayed in figure 11:

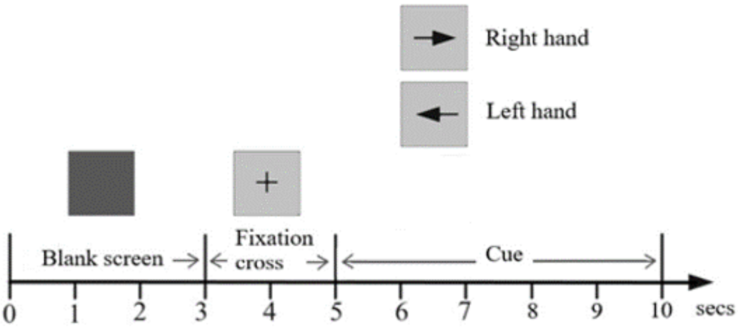

Figure 11: timeline of a single EEG trial.

6. A set of 20 trials are recorded continuously in one run which lasts less than 10 minutes
7. Depending upon the comfortability of the subjects, subsequent runs are conducted with sufficient breaks.
8. Before the start and after the end of each run, the physiological state of the subject is assessed using questionnaire. The questionnaire of all the subjects are attached in appendix section **??** and **??**.

Patients P01 and P03 completed one run whereas P02 completed 2 runs succesfully. Their mental and physical states were assessed using the questionnaires before and after each runs and the consolidated results are shown in figure 12. Patient P01's attentive level was not good as compared to the other patients. Patient P02 found the experiments exciting and was enthusiastic while doing the runs. Patient P03 was apprehensive at first due to the newness of the BCI setup but found the experiment session comfortable by the end of the run and took part in the experiment with good involvement.

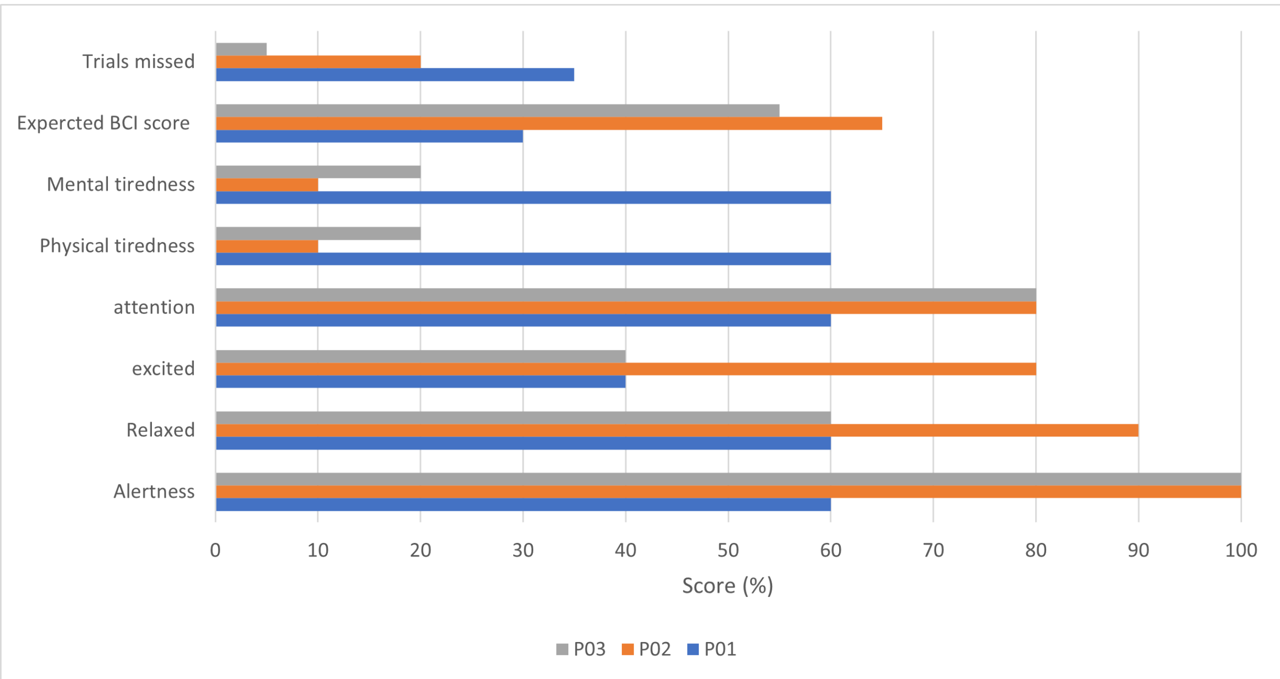

Figure 12: Patients psycho-physiological state assessment results.

- **Motor imagery results of MND patients:** The Time series and spectrogram plots of a random trial MI data during imagination period after the cue is illustrated in figure 13. The time series plot displays the voltage variation over time in collected over all the channels during the MI time period. The signal measured on the scalp are in the range of microvolts. The relevant frequency information for MI are in the range of 8-30Hz which includes the alpha and beta rhythms. Hence our data were filtered in this range before extracting the features.

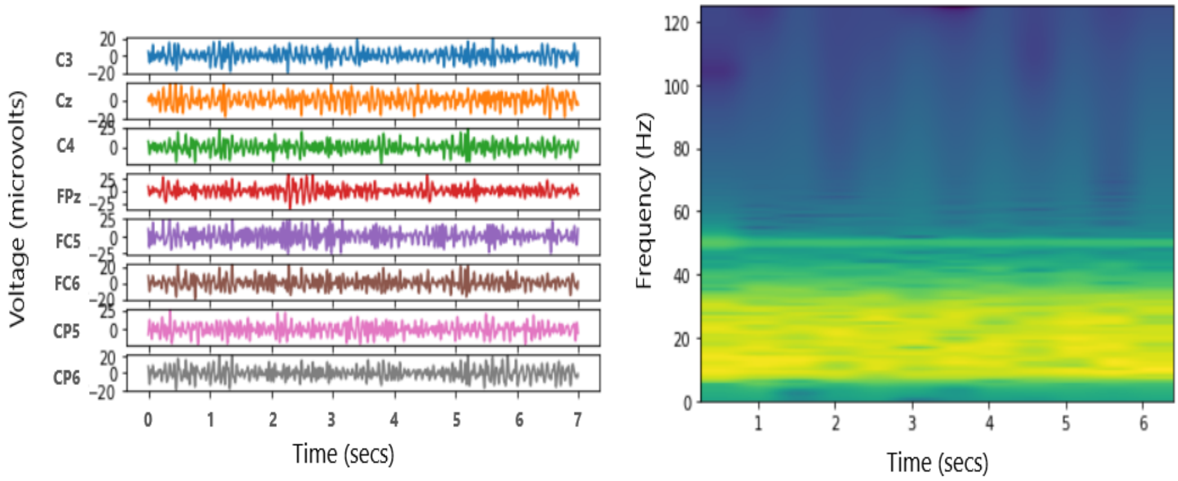

Figure 13: Time series and frequency spectrogram during MI.

We have evaluated the results of the patient's motor imagery experiments with 7 baseline classification pipelines. The pipelines comprises of both Riemannian based classifiers such as Minimum Distance to Mean (MDM), Fishers Geodesic MDM (FGMDM), Riemannian tangent space features with Support Vector Machine (SVM), Linear Discriminant analysis (LDA) and Common Spatial Pattern (CSP) features with to SVM and LDA classifiers. The classification accuracy results using these baseline classifiers are depicted in figure 14.

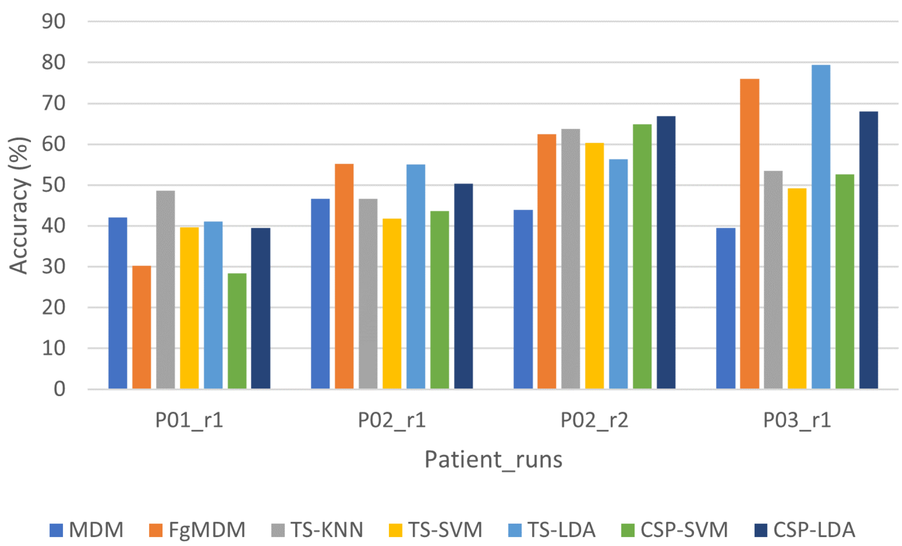

Figure 14: MI accuracy results of the MND patients.

The results show that P02's results improved by around 15% by the subsequent run as the patient became comfortable with the experiment protocol. Patient P01 showed lower performance because of his low attentive levels as observed in his psycho-physiological assessment through questionnaire. Patient P03 showed the best results among all the patients reaching an accuracy above 75% using Riemannian based FGMDM and TS-LDA classifiers. The reason of her reasonable good performance as compared to the other patients can be attributed to her age and also the extent of disability. These results and findings thus show promising potential for MI-BCI for movement disabled persons. In future, repetitive user training can be given to the patients and sufficient data can be collected to train our BCI setup for the robust operation of the autonomous wheelchair.

1.3 Objective 1.2: (b) Voice based control command generation and training models for voice to text.

- BCI and voice based testing done on healthy subjects.
- For deployment on an embedded arm64 compute device and for reliable offline classification of voice commands for goal selection, a dedicated voice to command model was developed and deployed.
- Goal selection was envisioned to be concluded via a guided user interface with voice commands to navigate the selection cursor. Directional commands like - 'up','down','left','right' were reserved for moving the cursor and 'select' was reserved for the confirm action. Commands 'stop', 'go' were reserved for emergency pause and resume. 'Back' was selected as an exit command, to exit the voice based menu to. Additionally, for ambient conversations and ambient noise, white noise was selected as a null class in order to differentiate between background conversations and voice triggers.
- Data was collected from 10 Individuals in order to better adapt to the indian demographic, and pronunciation Multiple sessional data was collected, and was augmented with white noise, ambient outdoor noise, and conversational background noise.
- After minimal pre processing, raw data was fed into a deep CNN based classifier as described in https://arxiv.org/pdf/1610.00087.pdf. Initially the standalone data was verified against the publicly available speech commands dataset, then a transfer learning approach was used to adapt the trained models to the target demographic.
- The model was adapted for use with Tensor RT, and optimised for deployment in jetson nano, a micro scale colette device drawing only 20 W of power and 2GB of RAM. The deployed integration of voice control alongside autonomous planning had a latency of 800ms while testing on a Jetson Nano device.

1.4 Objective 1.3: Fully manufactured system with design and electronic integration.

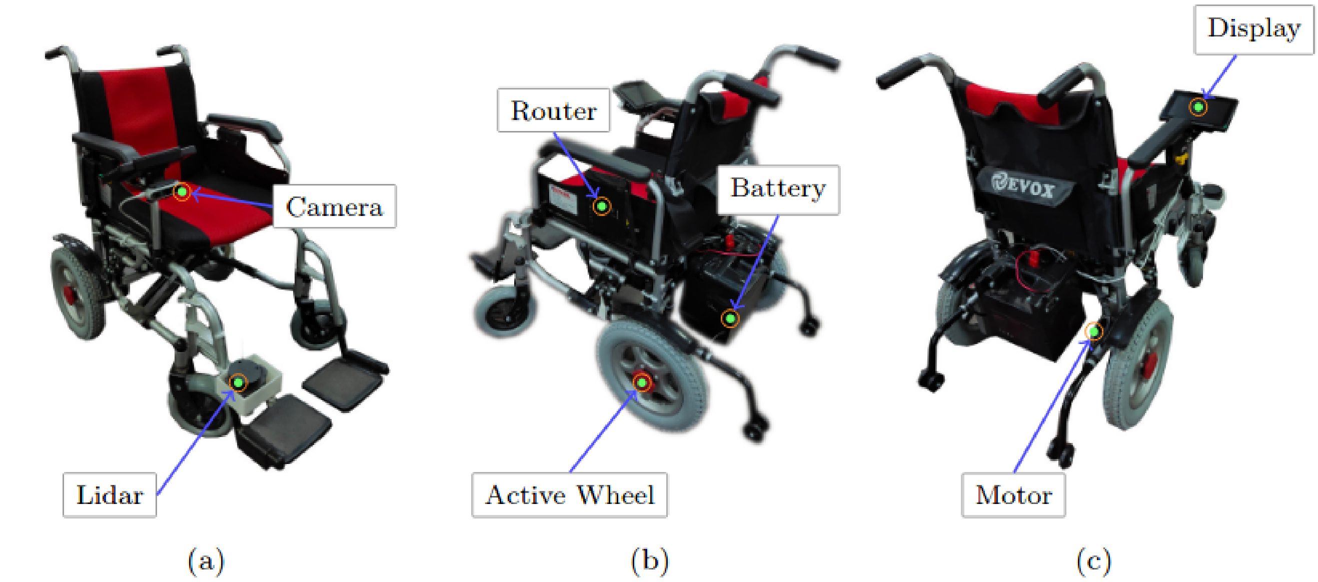

Figure 15: Component Placement.

2 Objective 2: Sensor Integration & Control module Testing in an indoor environment

Data from all the sensors are firstly fed into a data acquisition module, which generates all the transforms required according to location of different sensors. Data is then filtered to minimize errors. To get autonomous navigation setup, we need to get a map of the area. We are using *RTAB_MAP* to map the environment using *LiDAR* and depth cameras. The encoder and IMU are used to provide one of the odometry sources. Other odometry is generated by depth camera's point cloud and *LiDAR* scan. A 3D map was created[6]. This map and point cloud is saved in a local database to be used for localization. Localization is done *RTAB_MAP*, which takes point cloud database and match with the current local cloud to get an estimate of the position in the map.

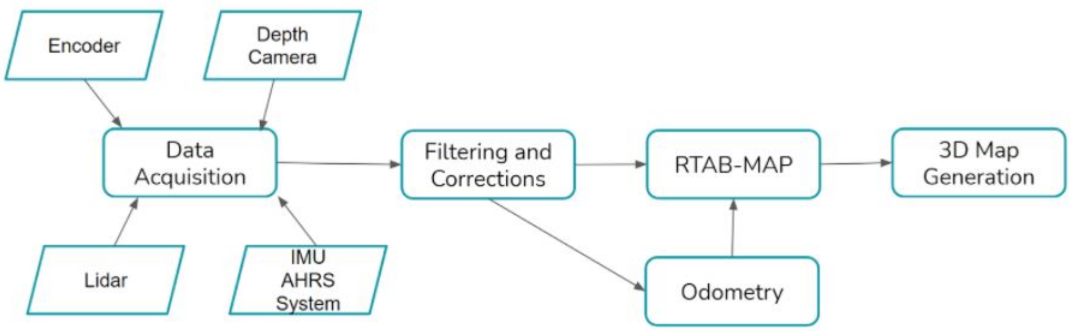

Figure 16: Mapping pipeline.

2.1 Obstacle Avoidance simulation and real-world testing:

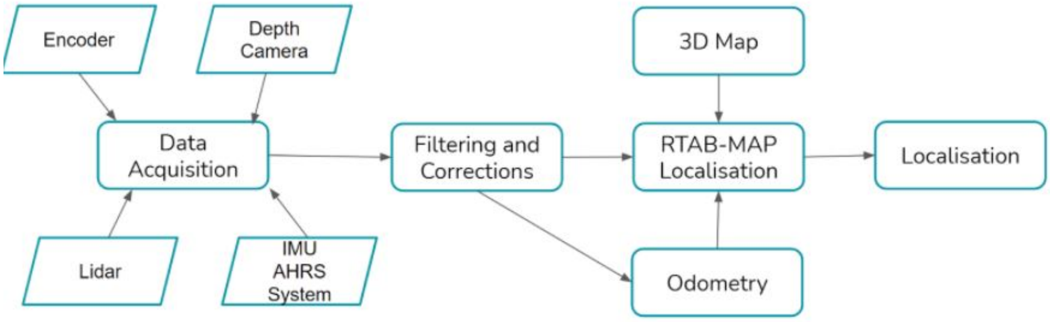

Figure 17: Localization pipeline.

2.2 Real-time testing of path-planning algorithms for Wheelchair.

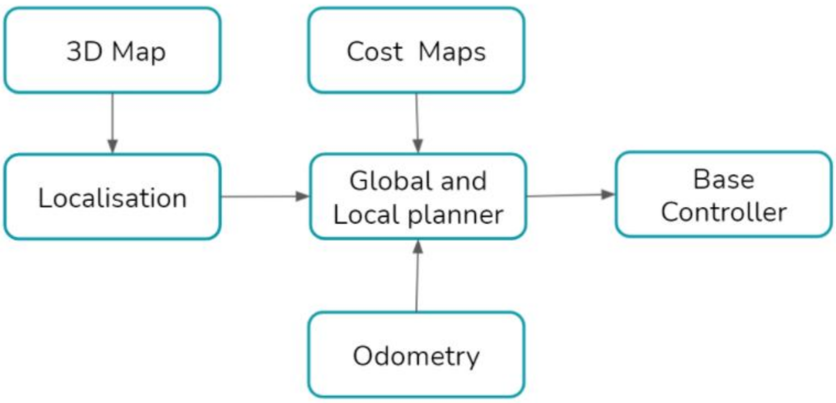

Figure 18: Autonomous path planning pipeline.

Once we have a map, real-time path-planning is achieved using Dijkstra's[7] and Dynamic Window Approach (DWA) path planners [8, 9] using cost maps and point clouds of obstacles. Path Planners generate a velocity command to the base controller, which controls individual wheels to move accordingly. A control loop is maintained to re-correct the localization. Goal is sent using a client which will later be replaced by a brain-controller client.

The Dijkstra algorithm is used as the global path planning algorithm and the DWA as its local path planning algorithm.

- Dijkstra's algorithm is one of the most used path planning algorithms, it seeks a feasible path starting from an initial position, searching in every direction for the goal position. Using a grid map, the vehicle can implement Dijkstra to find the goal prior to any movement.

- The DWA provides a controller that drives a mobile base in the plane. This controller serves to connect the path planner to the robot. Using a map, the planner creates a kinematic trajectory for the robot to get from a start to a goal location. Along the way, the planner creates, at least locally around the robot, a value function, represented as a grid map. This value function encodes the costs of traversing through the grid cells. The controller's job is to use this value function to determine velocities to send to the robot.

2.3 Environment for LAB Testing of the Autonomous Navigation and Path planning Module

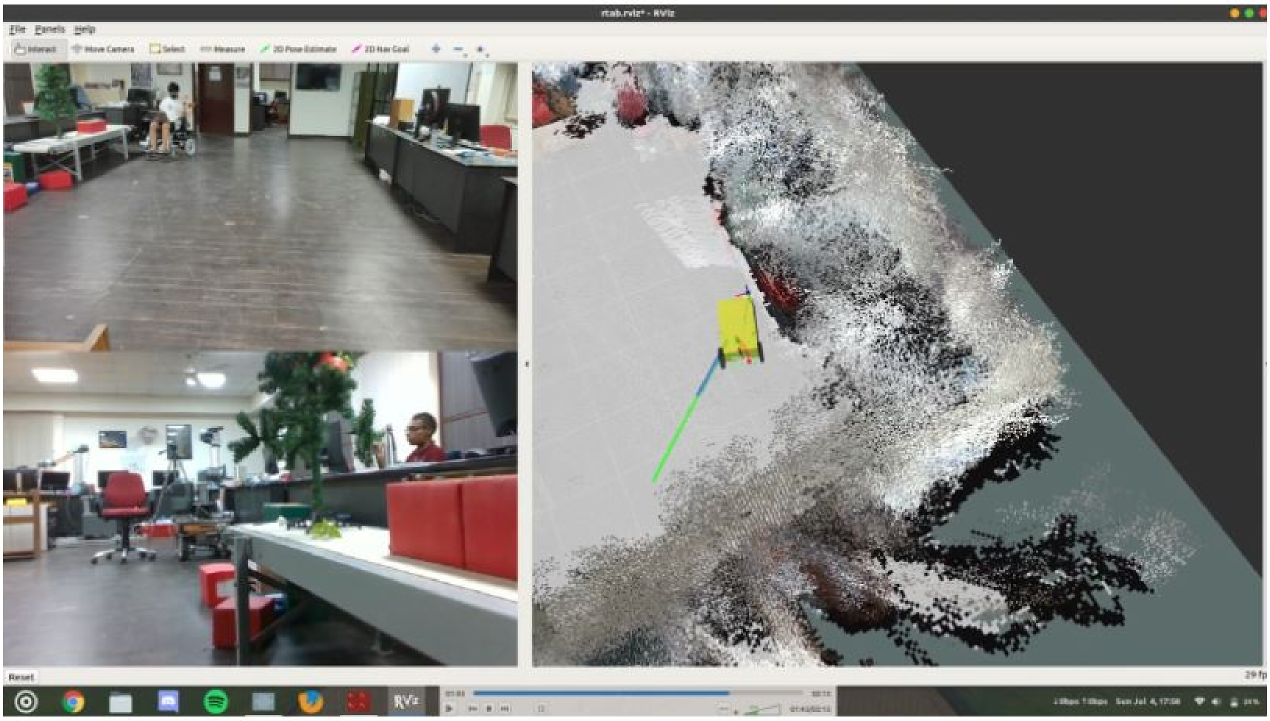

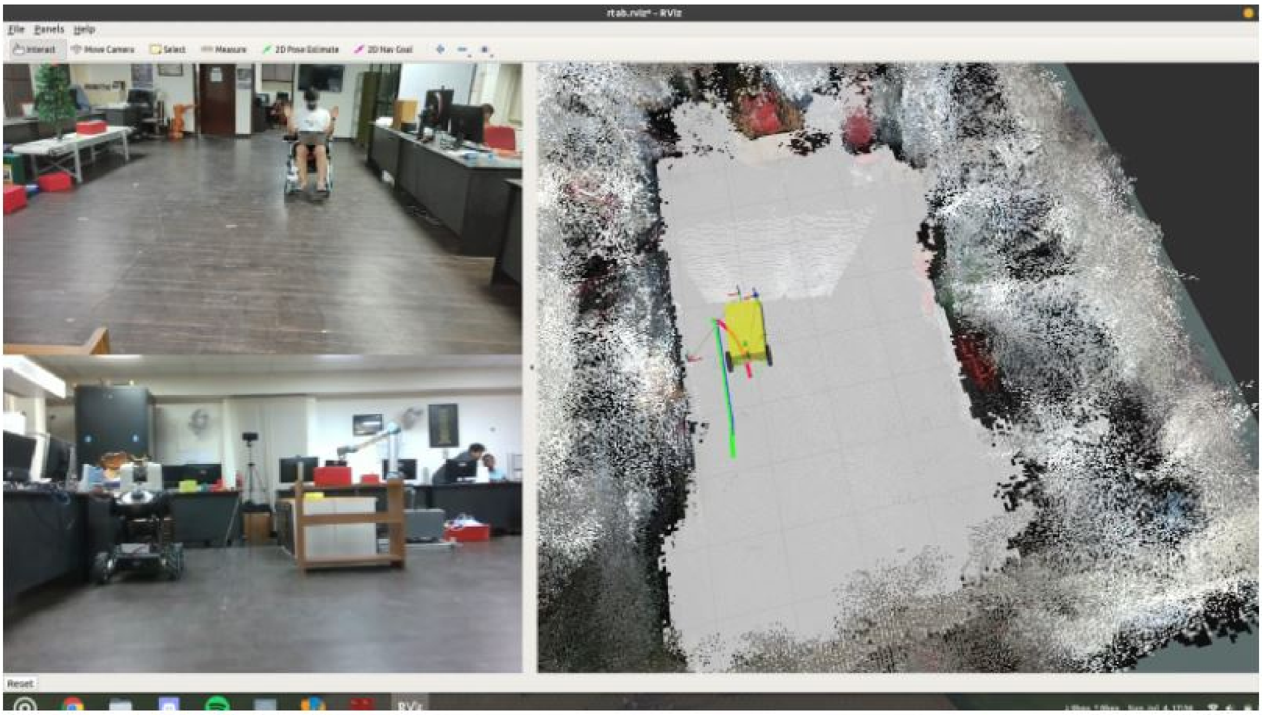

Figure 19: In the Images: Left top is camera feed from external camera, left bottom is camera feed from depth camera os the wheelchair, right frame is RVIZ view of 3D map Cloud of obstacles generated from depth camera and *RTAB_MAP*. These images are a snapshot of real-time autonomous navigation.

Link of video of Autonomous Navigation and Path Planning. https://youtu.be/xjp9DIsRWiQ.

2.4 Details of integration in simulated environment:

To implement the wheelchair virtual environment, Gazebo[10], and ROS were used. ROS is a meta-operating system for robots that includes hardware abstraction, low-level device control, implementation of commonly used functionality, message passing between processes, and package management. We used ROS because it can be easily integrated into other robot software frameworks, and many studies on robots has utilized ROS.

Using the building editor in Gazebo, a virtual indoor office environment of $10m \times 10m$ with a few obstacles was created. Fig. 20 shows the a virtual indoor office environment with obstacles. The right side figure present top view images of the environment in Fig 20. The square block A, and B indicate the two goal point of wheelchair, of which goal B is highlighted as it has been selected by the BCI user.

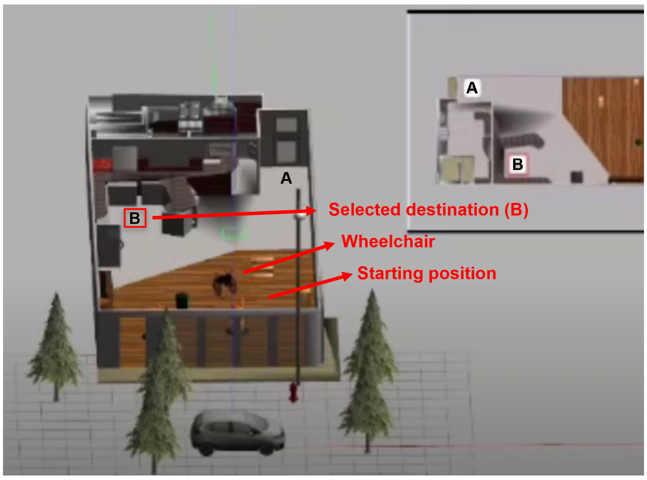

Figure 20: Testing of BCI prediction in virtual environment.

The YouTube link of the entire video sequence of BCI with virtual movement of wheelchair can be found in https://youtu.be/eM5FBEYDqIo. The BCI process starts with an instruction for the user to select a goal A or B. A focus cross $'+'$ is displayed for 2 secs to centre the attention of the user to the display. This is followed by the cue: left arrow (left hand imagination to select goal A) and right arrow (right hand imagination to select goal B). Based on his/her interest, the user selects his intended destination by performing the corresponding imagination action (in this case right hand imagination). The time for imagination is fixed to be 5 secs. The timeline for the focus cross and imagination are adapted in accordance with current trends in literature [11]. The online classification framework based on adaptive Riemannian geometry decodes the users intention by processing the 5 secs of EEG data during imagination and predicts the classification result (Goal B). This output is given as input to the simulated wheelchair which then moves autonomously to the selected destination (Goal B).

2.5 BCI controlled wheelchair

Goal is selected from the display GUI attached in the wheelchair using BCI module. Once the BCI module gives the final predication of goal, the autonomous path planning modules kicks in. The global planner, A^*[12] generates an efficient path according to the goal, and the DWA local planner ensures any dynamic change in the environment and obstacle avoidance. YouTube link can be found in https://photos.app.goo.gl/KR5soc9xd92d4baFA and https://youtu.be/_BZDbIu1nWY.

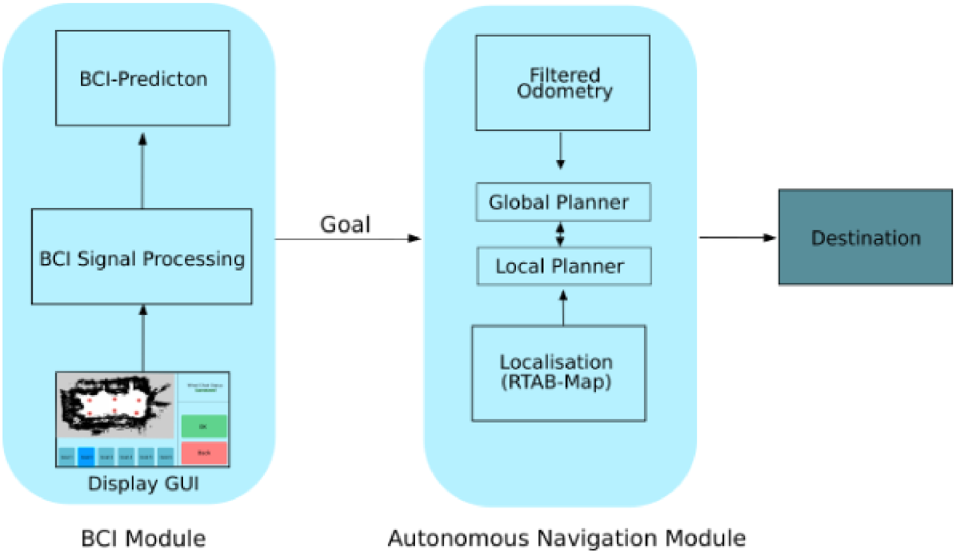

Figure 21: BCI integration with wheelchair.

Figure 22: Testing of BCI prediction in real environment.

Motion control system sets the velocities of wheels and odometry from the sensor fusion and localisation give feedback on pose and velocities. This loop continues until the wheelchair reaches its destination. If there is any fallback in any of the modules, recovery behaviours take control for the user's safety. After reaching the destination goal, it waits for the next goal.

3 Objective 3: Task Optimization and Multi-Scenario Testing

3.1 Outdoor Environment Testing

3.1.1 Mapping the Environment

Data from all the sensors are firstly fed which generates all the transforms required according to the location of different sensors. The transforms are necessary to relate different frames of reference, such as the laser frame, and base frame. To get an autonomous navigation setup, we need to get a map of the area. We are using Gmapping to map the environment using *LiDAR*. The Gmapping package provides a laser-based SLAM[13]. The wheel encoders are used to provide the odometry. A 2-D OGM is created. The pipeline of the creation of the map is given in figure 23. This package subscribes to the static transforms published along with the laser scan & wheel odometry data and publishes an occupancy grid map. This map is saved in a local database to be used for localization. The results of the real-world mapping can be found in https://youtu.be/3boluVXfzJI.

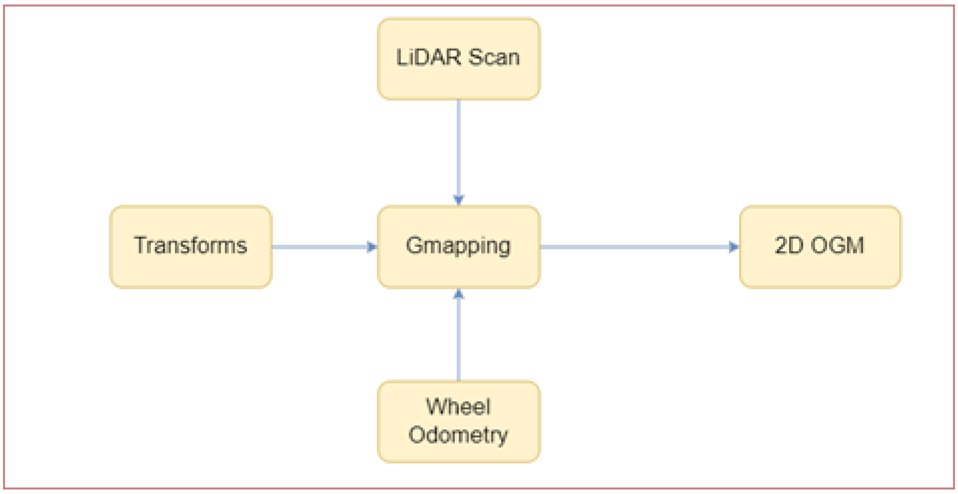

Figure 23: Mapping and navigation in outdoor environment.

3.1.2 Localisation & Path-Planning

Once we have a map, real-time path-planning is achieved using Dijkstra's and Dynamic Window Approach path planners using cost maps. Path Planners generate a velocity command to the base controller, which controls individual wheels to move accordingly. A control loop is maintained to re-correct the localization. Localization is done using AMCL. AMCL is a probabilistic localization system for a robot mapping a 2D environment. It implements the adaptive Monte Carlo localization approach which uses a particle filter to track the pose of a robot against a known map. The AMCL subscribes to the laser-based map, laser scans, and transform messages, and publishes the pose estimates. Path planning is achieved using the *move˙base* package. This package provides an implementation of an action that, given a goal in the world, will attempt to reach it with a mobile base. The *move˙base* node links together a global and local planner to accomplish its global navigation task. The goal is sent using a client which will later be replaced by a brain-controller client. The entire localization and autonomous navigation pipeline are given in figure 24. The outdoor environment consists of an open skywalk within the academic area of IIT Kanpur. The captured map of the outdoor environment by the wheelchair is shown in figure 25 The actual outdoor area is surrounded by brick wall of mid length height and has cement flooring with lots of tree cover. A snapshot of the image during outdoor wheelchair navigation is illustrated in figure 26. The demonstration of the wheelchair in an outdoor environment can be viewed in https://youtu.be/-IuF4PJl-5g.

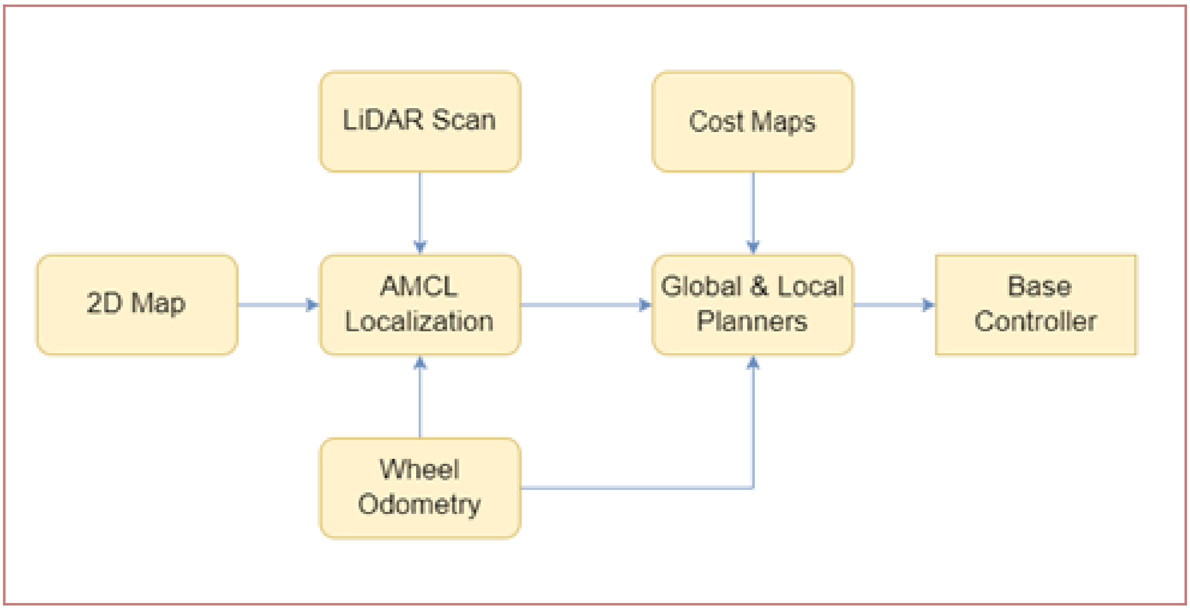

Figure 24: Localization & Autonomous Navigation Pipeline.

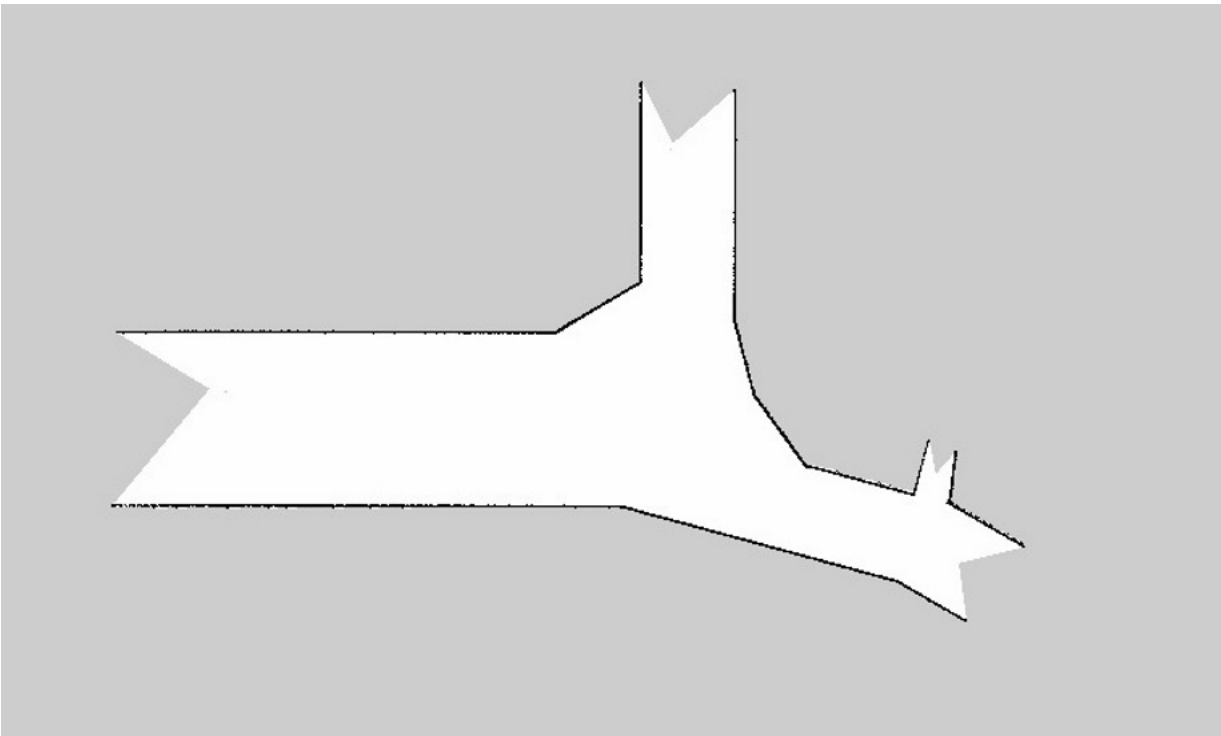

Figure 25: Outdoor environment.

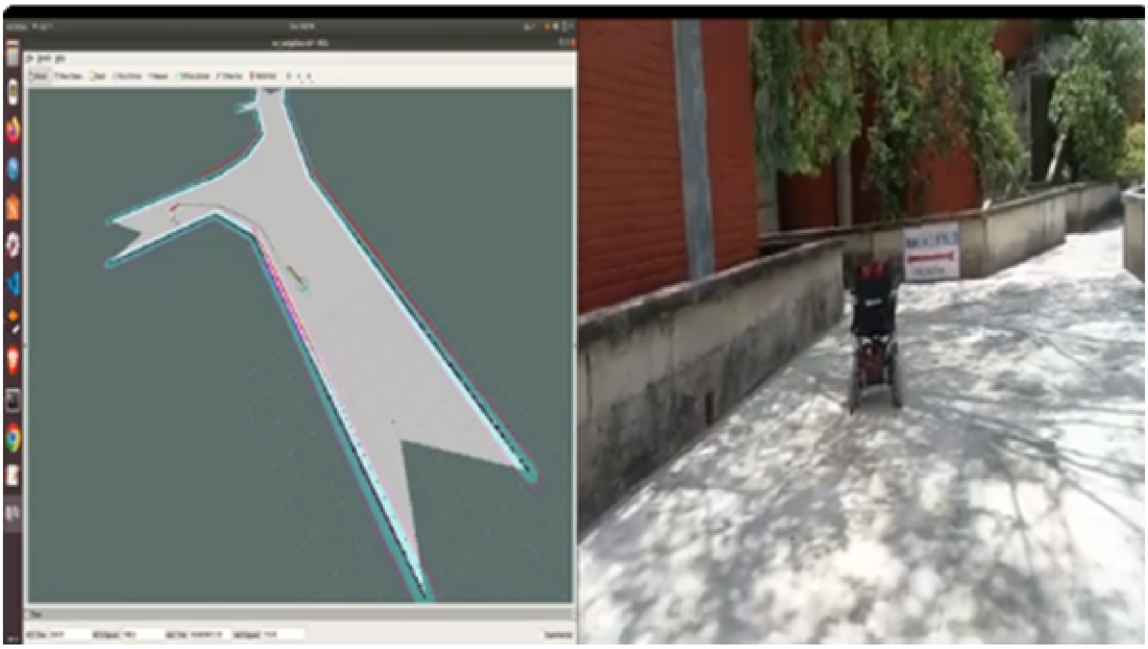

Figure 26: Mapping and navigation in outdoor environment.

4 Status of IP generation

- Autonomous wheelchair ready for patenting.
  - **Current status:** Patent meeting with the Research Establishment Officer, SIDBI Innovation & Incubation Centre (SIIC), IIT Kanpur has been conducted. As an outcome the meeting, we are in the process of filing the Invention Property Disclosure Format (IDPF) for the Brainwave controlled wheelchair.
- Brain-controlled module in process of getting integrated with the autonomous module.

5 Hardware Expenditure

The following important components are required for setup a autonomous wheelchair.

- EEG OpenBCI headset (1L).
- Power wheelchair (1.10L).
- Onboard PC (1.32L),
- RP Lidar (0.6L),
- Raspberry pi (0.45L),
- Motor driver (0.23L),
- Realsense camera (0.55L),
- NUC (1.25L).

It costs approximately Rs 6.50 lacs (without GST) to build an experimental wheelchair. This price can be reduced upto Rs 2.15 lacs (without GST) based on optimization of components costs.

6 Strategic product plans for the future

- The path planning and obstacle avoidance module can be incorporated in products which require optimized movement such as floor vacuum robot, robotic helpers (autonomous transporters) in hospitals etc.

Figure 27: Path planning in vacuum robot.

- We believe our approach's limitations are that key points have to be manually added within a known map by the developers/admins and then used by the user for BCI-based control. On the contrary, even in a newly realised map, the wheelchair can accept goal coordinates and orientation by manual touch entry. The roadblock limiting this higher level of freedom via BCI control is within the intent prediction models associated with BCI. Future work on enhancing the granularity in motor imaging estimates can allow for selecting any point in all maps (stored and realised) via BCI based input.
- The BCI and voice module can be incorporated into other assistive applications such as robotic arm which can also be integrated into the wheelchair. Such a system has the potential to assist even completely paralysed persons in performing their activities of daily living. As the robotic arm has more degrees of freedom to move than a wheelchair, we could explore the use of other imaginative tasks like mental calculation, mental recitation of poetry, imagination of 3D object rotation, object imagery etc to create differentiable brain patterns. The block diagram of such a futuristic setup is shown in figure 28. For decoding the brain signals in the BCI controlled robotic arm, We plan to incorporate our session independent adaptive framework for multi-class BCI (refer section 1.2.4) as the number of tasks required for classification will be greater in the case of robotic arm.

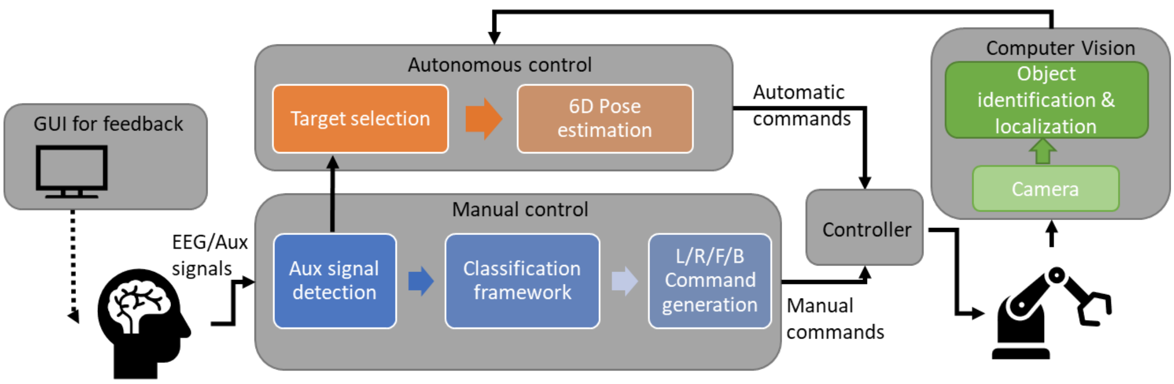

Figure 28: Robotic arm integrated into the wheelchair.

References

[1] Murat Köseoğlu, Murat Çelik Orkan, and Ömer Pektaş, "Design of an autonomous mobile robot based on ROS", *In 2017 International Artificial Intelligence and Data Processing Symposium (IDAP)*, pp. 1-5, 2017.

[2] L. Pillette, C. Jeunet, B. Mansencal, R. N'Kambou, B. N'Kaoua, F. Lotte, "A physical learning companion for Mental-Imagery BCI User Training ", *International Journal of Human-Computer Studies*, vol. 136, pp. 102380, 2020.

[3] J. Mladenovic, J. Frey, M. Joffily, E. Maby, F. Lotte, J. Mattout, "Active Inference as a Unifying, Generic and Adaptive Framework for P300-based BCI", *Journal of Neural Engineering*, vol. 17, no. 1, 0160542019, 2020.

[4] Fabien Lotte, Laurent Bougrain, Andrzej Cichocki, Maureen Clerc, Marco Congedo, Alain Rakotomamonjy, and Florian Yger. "A review of classification algorithms for EEG-based brain–computer interfaces: a 10 year update", *Journal of neural engineering*, vol. 15, no. 3, pp. 031005, 2018.

[5] Lotte, Fabien, "Signal processing approaches to minimize or suppress calibration time in oscillatory activity-based brain–computer interfaces.", *Proceedings of the IEEE*, vol. 103, no. 6, pp. 871-890, 2015.

[6] F. Endres, J. Hess, J. Sturm, D. Cremers, and W. Burgard, "3-D Mapping with an RGB-D Camera", *IEEE Transactions on Robotics*, vol. 30, no. 1, pp. 177–187, 2014.

[7] Lazaros C. Polymenakos, Dimitri P. Bertsekas, and John N. Tsitsiklis, "Implementation of efficient algorithms for globally optimal trajectories", *IEEE Transactions on Automatic Control*, vol. 43, no. 2, pp. 278-283, 1998.

[8] D. Fox, W. Burgard, and S. Thrun, "The dynamic window approach to collision avoidance", *IEEE Robotics Automation Magazine*, vol. 4, no. 1, pp. 23–33, 1997.

[9] Petter Ogren, , and Naomi Ehrich Leonard, "A convergent dynamic window approach to obstacle avoidance," *IEEE Transactions on Robotics*, vol. 21, no. 2, pp. 188-195, 2005.

[10] Kenta Takaya, Asai Toshinori, Kroumov Valeri, and Florentin Smarandache, "Simulation environment for mobile robots testing using ROS and Gazebo", *In 2016 20th International Conference on System Theory, Control and Computing (ICSTCC)*, pp. 96-101, 2016.

[11] H. Cho, M. Ahn, M. Kwon, & S. C. Jun, "A step-by-step tutorial for a motor imagery–based BCI", *In Brain–Computer Interfaces Handbook*, pp. 445-460, CRC Press, 2018.

[12] Liu, Xiang, and Daoxiong Gong, "A comparative study of A-star algorithms for search and rescue in perfect maze." *In 2011 international conference on electric information and control engineering*, pp. 24-27, 2011.

[13] Li, Yanyan, Nikolas Brasch, Yida Wang, Nassir Navab, and Federico Tombari, "Structure-SLAM: Low-drift Monocular SLAM in Indoor Environments", *IEEE Robotics and Automation Letters*, vol. 5, no. 4, pp. 6583-6590, 2020.